crystals

MDPI

Article

Enhanced Li^+ Ionic Conduction and Relaxation Properties of $Li_{5+2x}La_3Ta_{2-x}Ga_xO_{12}$ Garnets

Mohamad M. Ahmad [1,2,*], Fatimah R. Al-Ghareeb [1], Hicham Mahfoz Kotb [1,3], Sajid Ali Ansari [1], Tarek S. Kayed [4], Hassan A. Khater [1,3], Shalendra Kumar [1,5] and Koji Yamada [6]

1 Department of Physics, College of Science, King Faisal University, Hofuf 31982, Saudi Arabia; frg-14@hotmail.com (F.R.A.-G.); hkotb@kfu.edu.sa (H.M.K.); sansari@kfu.edu.sa (S.A.A.); hkhater@kfu.edu.sa (H.A.K.); sjagdish@kfu.edu.sa (S.K.)
2 Department of Physics, Faculty of Science, The New Valley University, El-Kharga 72511, Egypt
3 Physics Department, Faculty of Science, Assiut University, Assiut 71516, Egypt
4 Department of Basic Engineering Sciences, College of Engineering, Imam Abdulrahman Bin Faisal University, Dammam 34221, Saudi Arabia; tkayed@iau.edu.sa
5 Department of Physics, University of Petroleum and Energy Studies, Dehradun 248007, India
6 Department of Applied Molecular Chemistry, College of Industrial Technology, Nihon University, Narashino 275-8575, Japan; yamada.kouji@nihon-u.ac.jp
* Correspondence: mmohamad@kfu.edu.sa

Abstract: In the current work, we studied the effect of Ga^{+3} substitutions on the Ta^{+5} sites in $Li_{5+2x}La_3Ta_{2-x}Ga_xO_{12}$ (LLT-Ga) lithium conducting garnets (with x = 0.1–0.5) in order to enhance the ionic conductivity of these materials. The current materials are prepared by solid state reaction and their electrical properties are studied by impedance spectroscopy measurements. XRD data showed that cubic garnet phases are obtained for LLT-Ga garnets. The ionic conductivity increased by one order of magnitude for x = 0.3 composition with a value of ~4×10^{-5} S/cm compared to that of $Li_5La_3Ta_2O_{12}$ material. Moreover, the hopping frequency and the concentration of mobile Li^+ ions were estimated from analysis of the conductivity spectra, and it was found that both the concentration and mobility of Li^+ ions increased with increasing Ga^{+3} content in the materials. The dielectric and relaxation properties were studied in the dielectric permittivity and electric modulus formalisms. The current materials exhibited giant values of the dielectric constant of $\varepsilon' \sim 6500$, originating from internal effects in the materials.

Keywords: lithium conducting garnets; ionic conduction; conductivity relaxation; dielectric properties

check for updates

Citation: Ahmad, M.M.; Al-Ghareeb, F.R.; Kotb, H.M.; Ansari, S.A.; Kayed, T.S.; Khater, H.A.; Kumar, S.; Yamada, K. Enhanced Li^+ Ionic Conduction and Relaxation Properties of $Li_{5+2x}La_3Ta_{2-x}Ga_xO_{12}$ Garnets. *Crystals* **2022**, *12*, 770. https://doi.org/10.3390/cryst12060770

Academic Editor: Sergio Brutti

Received: 14 April 2022
Accepted: 23 May 2022
Published: 26 May 2022

Publisher's Note: MDPI stays neutral with regard to jurisdictional claims in published maps and institutional affiliations.

Copyright: © 2022 by the authors. Licensee MDPI, Basel, Switzerland. This article is an open access article distributed under the terms and conditions of the Creative Commons Attribution (CC BY) license (https://creativecommons.org/licenses/by/4.0/).

1. Introduction

Lithium-ion batteries are currently major power sources in our daily lives, where they are used in various electronic devices. [1,2]. Due to safety issues arising from organic electrolytes in modern batteries, there are appeals for the development of solid-state batteries using solid inorganic electrolytes. [3,4]. Several materials with good lithium ionic conductivity have been studied and lithium conducting garnet materials, $Li_5La_3M_2O_{12}$ (LLM, M = Ta or Nb) and $Li_7La_3Zr_2O_{12}$ (LLZ), are considered interesting materials due to their promising electrical properties [4–27]. LLM garnets have ionic conductivity of 10^{-6} S/cm at RT, whereas the ionic conductivity of LLZ reaches 10^{-4} S/cm at RT [4–16,18]. These garnet materials are purely ionic with negligible electronic conductivity [4–6,18]. Due to these promising properties LLZ garnets have attracted much research interest for possible applications as electrolytes in all solid-state batteries. LLZ could have a cubic (highly conductive) or tetragonal (poorly conductive) phase. The cubic phase is stabilized by high temperature sintering above 1200 °C. However, this high temperature sintering is usually associated with Al contamination from the alumina crucibles. It is found that Al-substitution on Li sites is the reason for the stabilization of the cubic phase of LLZ.

The ionic conductivity of LLZ could be enhanced by chemical substitutions, either in the Li sites, by AL^{+3}, Ga^{+3}, Y^{+3}, or in the Zr sites, by higher valency cations, such as Ta^{+5}, Nb^{+5}, Te^{+6} and W^{+6}, leading to ionic conductivity >10^{-3} S/cm [18–25]. The ionic conductivity of 10^{-6} S/cm at RT of LLT is relatively low, leading to extensive research efforts to improve the ionic conductivity of these materials. Chemical substitutions by divalent/trivalent cations on the La^{+3}/Ta^{+5}, such as in $Li_6ALa_2Ta_2O_{12}$, A = Ba, Ca, Sr, Mg, [2–9] and in $Li_{5+2x}La_3Ta_{2-x}Y_xO_{12}$ [13], lead to enhanced ionic conductivity to 10^{-5}–10^{-4} S/cm at RT [5–13]. Other factors could also influence the ionic conductivity of garnet materials including the preparation techniques and processing conditions, such as the calcinations temperature and sintering steps [4–14]. Chemical substitution by divalent cations on the La sites, or trivalent cations on the Ta sites, in LLT garnets, will increase the lithium content in the materials, leading to increasing ionic conductivity.

Until now, there are no studies on the effect of Ga^{+3} substitutions on ionic conduction in LLT garnets. Moreover, most of the research work on ionic conduction in garnets is performed at ambient and high temperatures, and few low temperature studies have been reported. Low temperature measurements are expected to help in understanding the conduction and relaxation properties of garnet materials. Moreover, the presence of high-density mobile Li^+ ions could induce dielectric dipoles, leading to high values of the dielectric constant. Therefore, the aims of the present work are: (i) synthesis of $Li_{5+2x}La_3Ta_{2-x}Ga_xO_{12}$ (LLT-Ga; x = 0.1–0.5) lithium conducting garnets in order to enhance lithium ionic conductivity, (ii) study of the relaxation dynamics in garnet materials through analysis of the electric modulus spectra at different temperatures, and (iii) exploring the dielectric properties of LLT-Ga garnets.

2. Materials and Methods

$Li_{5+2x}La_3Ta_{2-x}Ga_xO_{12}$ (with x = 0.1, 0.2, 0.3, 0.4, 0.5; all the samples LLT-Ga1, LLT-Ga2, LLT-Ga3, LLT-Ga4 and LLT-Ga5, respectively) have been synthesized by mechanical milling and solid-state reaction techniques. High purity Li_2CO_3, La_2O_3, Ta_2O_3 and Ga_2O_3 were used. Excess 10 wt% of Li_2CO_3 was added for compensation of Li_2O. The mixed powder was ball milled for 12 h with 250 rpm. The resulting powder was calcined at 700 °C for 12 h, then ball milled again under the same conditions. A second calcination step was performed at 900 °C for 12 h followed by final milling at 400 rpm for 3 h. The ball milling steps were performed in 2-propanol using Fritsch P-7 premium line machine with 45 mL pots and 14 balls of 10 mm diameters, both made from tungsten carbide. The balls to powder mass ratio was 8:1. The obtained powder was pressed under 2.5 ton in a 10 mm diameter die to get pellets with a 1–2 mm thickness. The sintering of the samples was performed at 1000 °C for 12 h in alumina crucibles. To prevent possible Al contamination of the samples during the sintering process in alumina crucibles the pellets were buried in a large quantity of the powder to prevent direct contact of the pellets with the alumina crucibles. Structural characterization of LLT-Ga samples was studied by XRD measurements in the $10 \leq 2\theta \leq 80$ range using monochromated radiation (λ = 1.5406 Å) with a step of 0.02° using a Bruker D8 advance diffractometer. SEM measurements were performed with a field emission scanning electron microscope, Joel SM7600F, to determine the grain size of the materials. The electrical and dielectric properties of LLT-Ga samples were studied by impedance spectroscopy. Silver paste was applied on both surfaces of the sintered pellets as electrodes. The impedance data were collected in the 1–10^7 Hz frequency range at different temperatures using the Novocontrol concept 50 system.

3. Results and Discussion

The XRD patterns of LLT-Ga samples are shown in Figure 1. The observed patterns in Figure 1 agree with the standard XRD database of $Li_5La_3Ta_2O_{12}$ (PDF#45-0109), indicating the formation of the cubic garnet structure. Minor impurity peaks are also observed in the XRD patterns of these materials. The Rietveld refinement method was deployed using

RIETAN-2000 software [28] for the investigated materials in order to elucidate the lattice parameters of the materials.

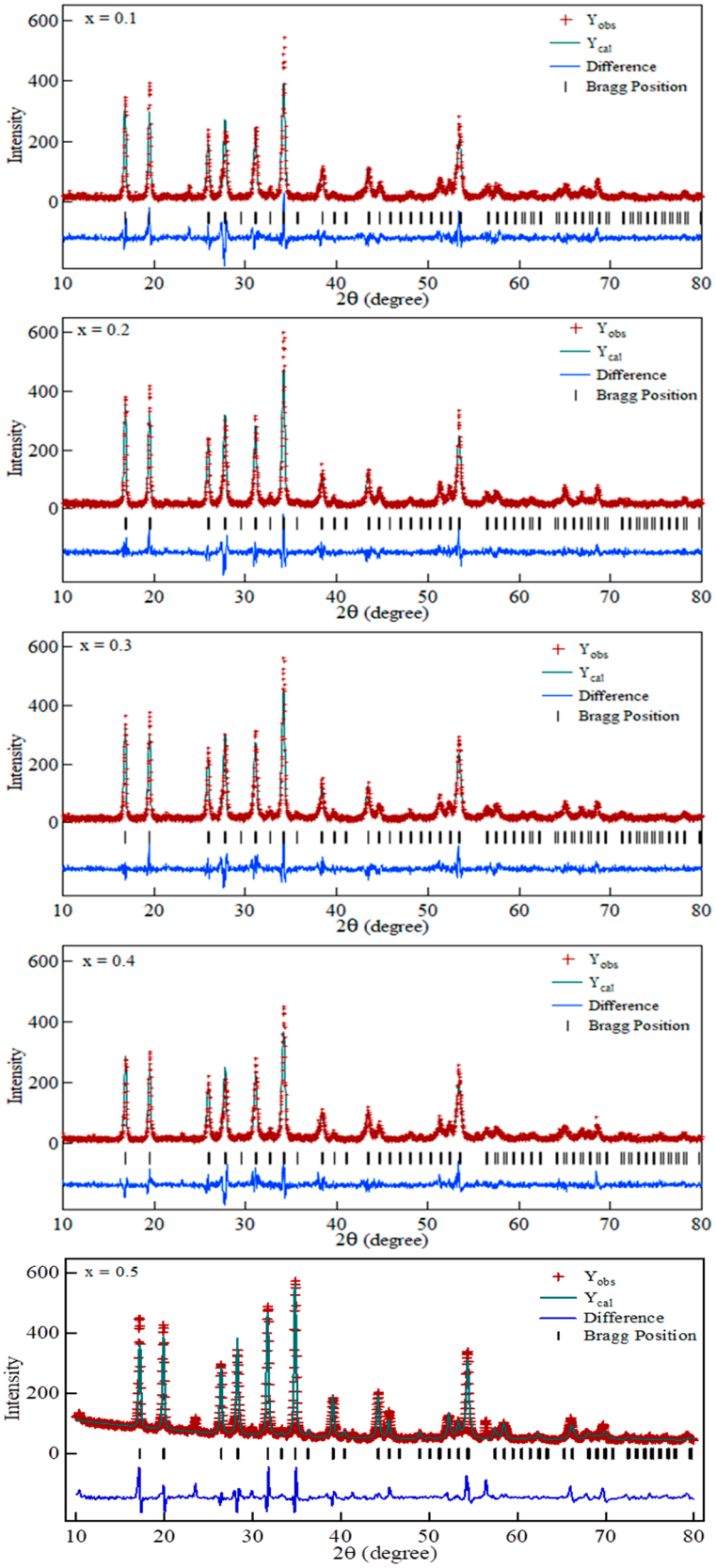


Figure 1. Rietveld refinement of XRD data of $Li_{5+2x}La_3Ta_{2-x}Ga_xO_{12}$ garnets.

The results in Figure 1 indicate that LLT-Ga samples have cubic structure with the space group $Ia\bar{3}d$ with an average lattice constant of 12.827 Å for x = 0.1–0.5 samples. The value of the lattice constant of the current LLT-Ga garnets agrees well with the value of 12.85 Å reported previously for LLT samples prepared by the sol-gel technique [14]. Moreover, we noticed that there was no change in the lattice constant with increasing Ga^{+3} content due to the close matching between the ionic radius of Ga^{+3} (0.62 Å) with that of Ta^{+5} ions (0.64 Å). In Figure 1 we notice the presence of impurity peaks in the XRD patterns. One major impurity peak was observed in x = 0.1 sample at 23.8°, whereas the impurity content increased for x = 0.5 sample, as evidenced by the presence of several impurity peaks at 23.5°, 29.9°, 41.2°, 42.5° and 56.2°. The impurity phases could be assigned to $LiGaO_2$ (PDF# 72-1640) and La_2O_3 (PDF# 74-1144). SEM micrographs for LLT-Ga ceramics are shown in Figure 2. Dense ceramics with well-defined coarse grains were obtained for all Ga^{+3} compositions, with grain size in the 3–5 µm range. It can be observed in Figure 2 that no noticeable changes in the grain size or the morphology of the ceramics were observed with increasing Ga^{+3} substitutions in the materials.

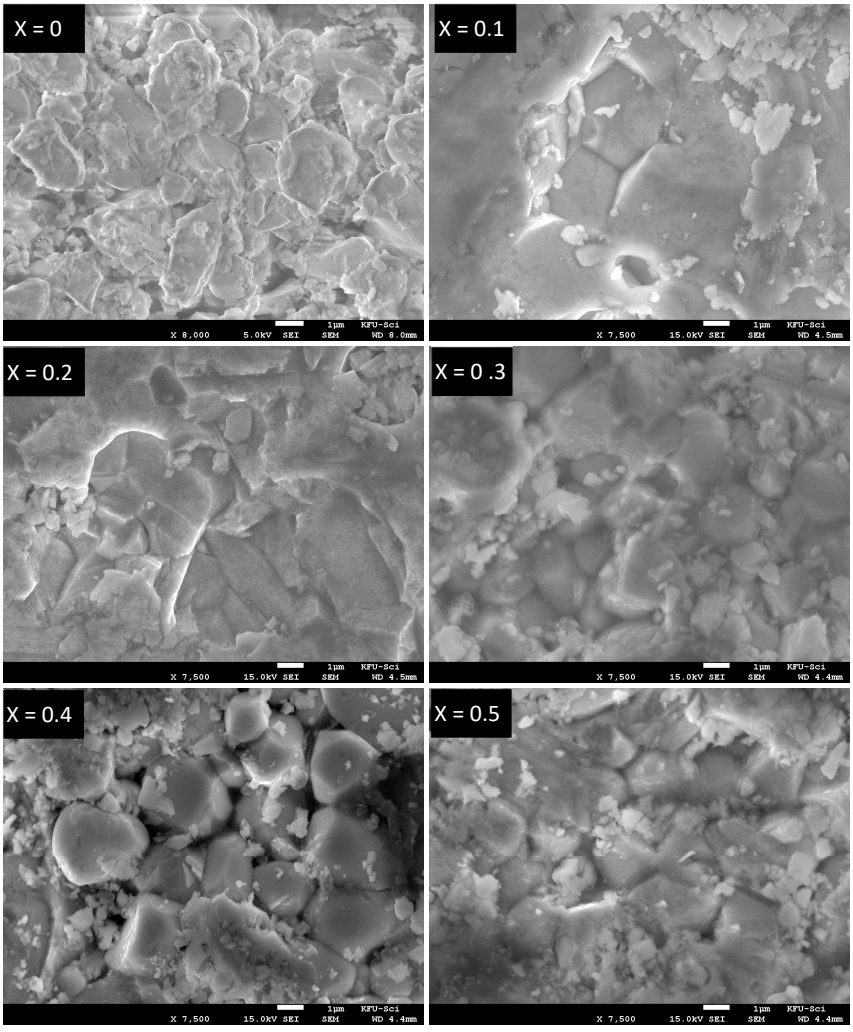


Figure 2. SEM micrographs of $Li_{5+2x}La_3Ta_{2-x}Ga_xO_{12}$ ceramics with different Ga^{+3} compositions.

Impedance diagrams of LLT-Ga3 ceramics are shown in Figure 3 as a representative example. A single semicircle at the high frequency region is observed, where the effect of the grain boundaries could not be distinguished in this figure. Therefore, the real axis intercept of the semicircles represents the total resistance, R, of the materials. The total ionic conductivity was calculated by the relation; $\sigma_{dc} = l/RA$, where l is the sample thickness and A is the surface area. The variation of the lithium ionic conductivity of LLT-Ga ceramics

with temperature is depicted in Figure 4, where the conductivity follows the Arrhenius relation;

$$\sigma_{dc} = \sigma_o \exp\left(-\frac{\Delta E}{kT}\right) \quad (1)$$

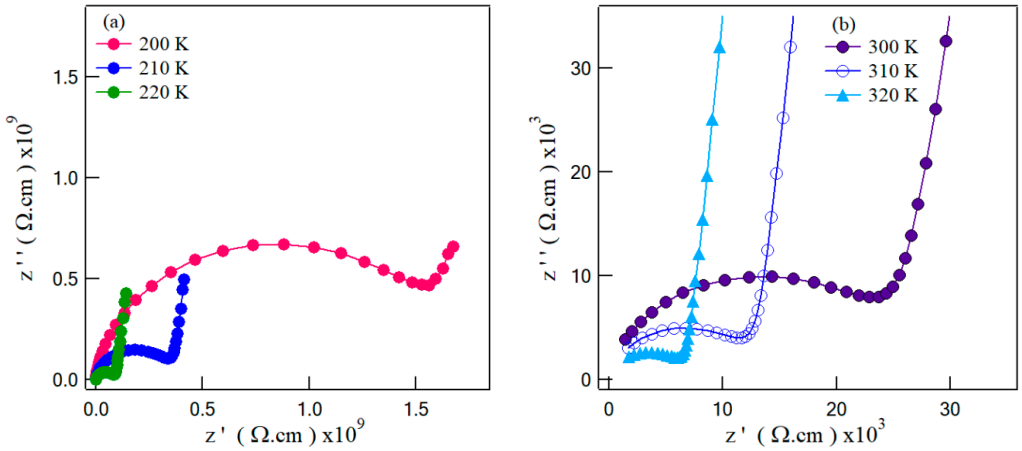


Figure 3. Complex impedance diagrams at selected temperatures for $Li_{5.6}La_3Ta_{1.7}Ga_{0.3}O_{12}$ garnets at (**a**) low and (**b**) high temperature regions.

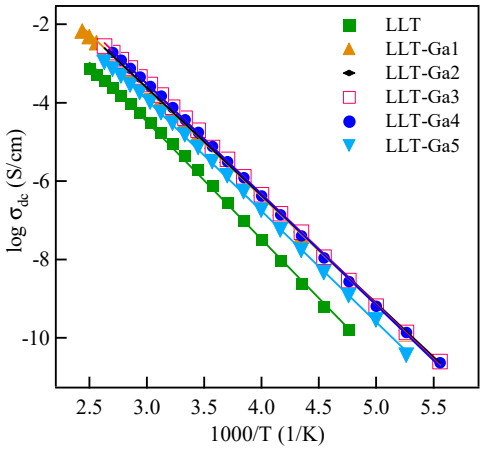


Figure 4. The temperature dependence of the total ionic conductivity for different compositions of $Li_{5+2x}La_3Ta_{2-x}Ga_xO_{12}$ garnets along with the pure $Li_5La_3Ta_2O_{12}$.

The values of σ_{dc} at 300 K of $Li_{5+2x}La_3Ta_{2-x}Ga_xO_{12}$ ceramics are summarized in Table 1. It is clear that the $Li_{5.6}La_3Ta_{1.7}Ga_{0.3}O_{12}$ garnets exhibited the highest conductivity with a value of 4×10^{-5} S/cm compared to 4.26×10^{-6} S/cm of pure $Li_5La_3Ta_2O_{12}$, indicating considerable lithium conductivity enhancement is achieved by Ga^{+3} substitutions in LLT garnets. It is clear from Figure 4 and the data in Table 1 that the most effective doping region was up to x = 0.1 of Ga^{+3} content, where for larger Ga^{+3} content, between x = 0.2–0.4, the conductivity was almost saturated. On further increase in Ga^{+3} content (i.e., for x = 0.5) conductivity dropped slightly, due to the increased content of impurity phases in this composition. The activation energy of conduction equaled 0.55 eV for all LLT-Ga samples, which is comparable to that of pure LLT garnets of 0.55–0.60 eV [5,14].

Table 1. The values of σ_{dc} at 300 K and the activation energy ΔE for ionic conduction of $Li_{5+2x}La_3Ta_{2-x}Ga_xO_{12}$ garnets. E_σ and E_H are the activation energy for the conduction and the hopping process, whereas $E_{tan\delta}$ is the activation energy of the dielectric relaxation process determined from dissipation factor. n_c is the average value of the concentration of Li^+ mobile ions.

x	σ_{dc} at 300 K (S/cm)	ΔE (e.V)	E_σ (e.V)	E_H (e.V)	$E_{tan\delta}$ (e.V)	n_c (cm^{-3})
0.00	4.26×10^{-6}	0.62	0.62	0.55	0.51	9.10×10^{20}
0.10	3.21×10^{-5}	0.55	0.53	0.47	0.55	1.23×10^{21}
0.20	3.13×10^{-5}	0.55	0.52	0.46	0.54	1.31×10^{21}
0.30	4.00×10^{-5}	0.56	0.53	0.47	0.57	1.21×10^{21}
0.40	3.68×10^{-5}	056	0.53	0.47	0.57	1.62×10^{21}
0.50	1.50×10^{-5}	0.56	0.55	0.52	0.56	9.92×10^{20}

According to the chemical formula $Li_{5+2x}La_3Ta_{2-x}Ga_xO_{12}$ of Ga^{+3} substituted garnets the Li^+ content per unit formula was expected to increase from 5Li in pure LLT to (5 + 2x)Li for x content of Ga^{+3}. The increased content of Li^+ ions could be the reason for the enhanced conductivity of Ga substituted LLT materials. Furthermore, Ga^{+3} substitutions in LLT-Ga materials may create accessible vacant sites for Li^+ ions, which enhance mobility and conductivity. In the following, we will estimate the hopping frequency (ω_H) and the concentration (n_c) of mobile Li^+ ions in LLT-Ga garnets. The conductivity spectra of LLT-Ga3 ceramics are shown in Figure 5. A frequency independent dc conductivity was observed at low temperatures and frequencies, followed by a dispersion region where $\sigma'(\omega)$ increased with frequency at the high frequency range. The conductivity data were analyzed by the following formula [29–32],

$$\sigma'(\omega) = \sigma_{dc}\left[1 + \left(\frac{\omega}{\omega_H}\right)^n\right] \quad (2)$$

and the *dc* conductivity in Equation (2) could be expressed as:

$$\sigma_{dc} = en_c\mu = \frac{n_c e^2 \gamma \lambda^2}{kT}\omega_H \quad (3)$$

In the above equations n represents the exponent of the dispersion region of the conductivity, $\gamma = 1/6$ is a geometrical factor for 3D ion hopping and λ is the hopping distance. The fitting results of the conductivity spectra are shown in Figure 5, and the temperature variation of the estimated parameters σ_{dc} and ω_H is shown in Figure 6. The values of the activation energy for the conduction, E_σ, and the hopping process, E_H, were almost the same [see Table 1]. The values of n_c for mobile Li^+ ions in LLT-Ga ceramics were estimated [see Table 1] using Equation (3) with a value of λ = 1.7 Å [33]. The values of n_c increased by a factor of ~1.8 after Ga substitutions in LLT-Ga garnets. On the other hand, the hopping frequency of Li^+ ions increased considerably as Ga^{+3} content increased up to x = 0.3 [see Figure 6]. These observations suggest that enhanced Li^+ ionic conductivity in LLT-Ga ceramics is due to the increased concentration and mobility of Li^+ ions up to x = 0.3 of Ga^{+3} content. For x = 0.4 and 0.5 compositions, the hopping frequency decreased leading to a decrease in ionic conductivity. This drop in the hopping frequency could be attributed to the increased content of impurity phases in the materials.

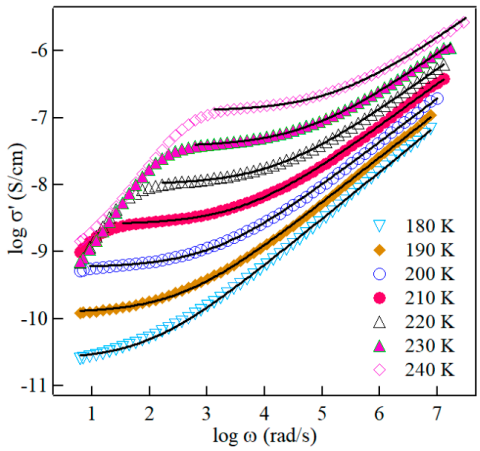


Figure 5. The conductivity spectra of LLT-Ga garnets with x = 0.30 at different temperatures. The solid curves between the points represent the best fits to Equation (2).

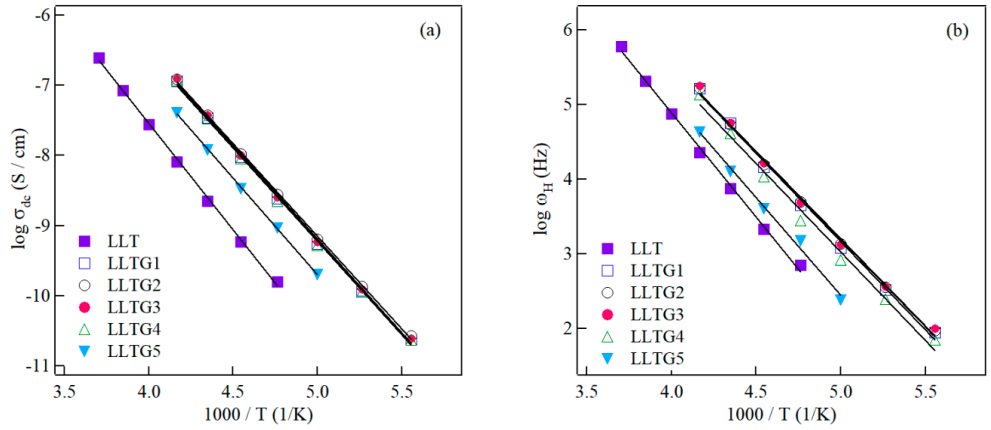


Figure 6. (**a**) The temperature dependence of the dc conductivity, σ_{dc}, and (**b**) the hopping frequency, ω_H, as determined from the fitting process in Figure 5.

In garnet structure Li^+ ions could occupy either the immobile 24 d tetrahedral Li(1) sites or the mobile 48 g/96 h octahedral Li(2) sites [15,16]. The occupancy of Li^+ ions in these sites depends on the total Li^+ content per unit formula in the material. If Li^+ content is low (3Li in $Li_3Nd_3Te_2O_{12}$ for example), Li^+ ions will occupy all the immobile Li(1) sites and the Li(2) sites are kept empty, leading to poor ionic conductivity. For garnet materials with higher Li^+ content, such as in LLT (5Li per unit formula), our current materials LLT-Ga [(5 + 2x)Li per unit formula] or LLZ (7Li per unit formula), redistribution of Li^+ occupancy occurs where the occupancy of the tetrahedral Li(1) sites decreases and occupancy of the octahedral Li(2) sites increases [15,16]. This redistribution process leads to more vacant Li(1) sites which become accessible for the movement of Li^+ ions and facilitate the 3D diffusion pathway of Li^+ through 24 d-96 h-48 g-96 h-24 d chain [26,27]. Therefore, the observed enhancement of the ionic conductivity in LLT-Ga is due to both increasing concentration and hopping frequency (i.e., the mobility) of mobile Li^+ ions with Ga^{+3} substitution in the materials.

Different classes of materials, including ferroelectrics, perovskite oxide dielectrics and ionic conductors, exhibit giant dielectric constant [34–38]. The frequency dependence of the dielectric constant ε' for $Li_{5.2}La_3Ta_{1.9}Ga_{0.1}O_{12}$ garnets is shown in Figure 7a. A plateau region with $\varepsilon' \sim 6500$ was observed at low frequencies, whereas the high frequency plateau represented the bulk effect with $\varepsilon' \sim 35$. Nyquist plots of the dielectric data at 280 K are shown in Figure 7b. In this figure, three contributions can be distinguished. At high frequencies the value of the dielectric constant was $\varepsilon' \sim 35$ [inset of Figure 7b], which corresponded to the grain dielectric permittivity. A large semicircle with a value of $\varepsilon' \sim 6500$ was observed in the intermediate frequency region followed by a spike at lower frequencies.

The observed spike in Figure 7b could be due to the electrode polarization effect at the sample-electrode interface region. Therefore, the high value of $\varepsilon' \sim 6500$ could originate from other internal effects in the materials, such as the formation of dipolar polarization due to the displacement of Li^+ ions in the octahedral, similar to $Li_{5+2x}La_3Ta_{2-x}Y_xO_{12}$ [13]. ε' spectra of all LLT-Ga ceramics at 300 K are shown in Figure 7c for comparison. All of the investigated ceramics exhibited similar dielectric response with giant dielectric constant values. The spectra of tan δ (tan $\delta = \varepsilon''/\varepsilon'$) for x = 0.10 composition is shown in Figure 8 at selected temperatures. The relaxation time, calculated from the peak frequency of tan δ spectra, and its temperature dependence are shown in Figure 8. The values of the activation energy of the dielectric relaxation process are summarized in Table 1, which agree with activation of the ionic conduction process.

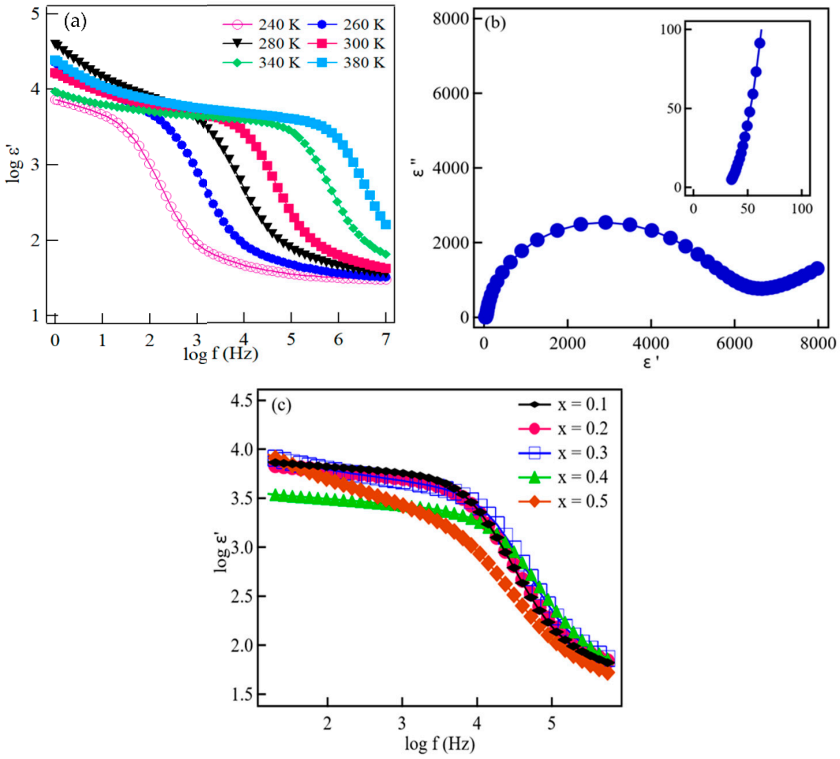


Figure 7. (**a**) ε' spectra for LLT-Ga1 at selected temperatures as a representative sample and (**b**) the Cole-Cole diagram at 280 K for LLT-Ga1 with the inset showing high magnification of the high frequency region. (**c**) ε' spectra for all $Li_{5+2x}La_3Ta_{2-x}Ga_xO_{12}$ compositions at 300 K.

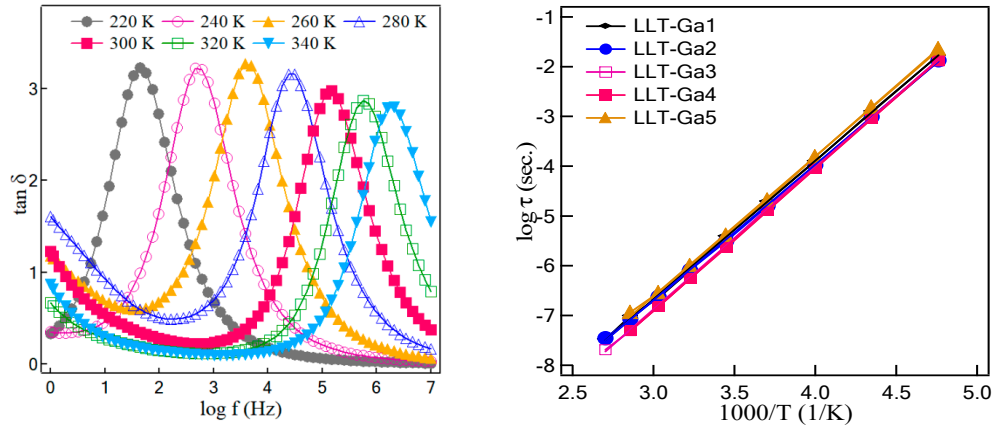


Figure 8. (**a**) The frequency dependence of tan δ for LLT-Ga1 as a representative example, and (**b**) the temperature dependence of the dielectric relaxation time of $Li_{5+2x}La_3Ta_{2-x}Ga_xO_{12}$ garnets.

4. Conclusions

In the present work we successfully synthesized $Li_{5+2x}La_3Ta_{2-x}Ga_xO_{12}$ lithium conducting garnets with cubic structure. Impurity phases became more prominent for higher content of $Ga^{+3} \geq 0.40$. The ionic conductivity of the Ga substituted garnets was one order of magnitude larger than that of pure LLT materials, with x = 0.30 composition exhibiting the highest conductivity of 4–10^{-5} S/cm at 300 K. We estimated the values of the hopping frequency and the concentration of mobile Li^+ ions in the investigated materials. It was concluded that the enhanced ionic conductivity in LLT-Ga garnets is due to increasing both the concentration and mobility of Li^+ ions in the materials, with mobility having a more prominent role. The relaxation properties of the investigated materials were studied through dielectric permittivity formalisms. The dielectric relaxation time from the dissipation factor was determined and found to be thermally activated with the same activation energy of the conduction process. This result indicates that Li^+ ions are responsible for long-range transport as well as the local re-orientation relaxation in garnet materials. The current materials exhibited giant dielectric values of $\varepsilon' \sim 6500$, which were not related to surface polarization at the sample/electrode interface.

Author Contributions: Conceptualization, M.M.A.; methodology, M.M.A., F.R.A.-G. and H.M.K.; validation, M.M.A. and H.M.K.; formal analysis, M.M.A., F.R.A.-G., H.M.K., S.K. and K.Y.; investigation, M.M.A., F.R.A.-G., H.M.K., S.A.A., T.S.K. and H.A.K.; resources, M.M.A. and H.M.K.; data curation, M.M.A., H.M.K. and K.Y.; writing—original draft preparation, M.M.A.; writing—review and editing, H.A.K. and S.A.A.; supervision, M.M.A. and H.M.K.; project administration, H.M.K.; funding acquisition, H.M.K. All authors have read and agreed to the published version of the manuscript.

Funding: This research was funded by the Deanship of Scientific Research in King Faisal University (Saudi Arabia), grant number 1811017 and the APC was funded by the same grant number 1811017.

Institutional Review Board Statement: Not applicable.

Informed Consent Statement: Not applicable.

Data Availability Statement: The data presented in this study are available in the article.

Acknowledgments: The authors acknowledge the Deanship of Scientific Research at King Faisal University (Saudi Arabia) for financial support under the Research Group Support Track (grant number 1811017).

Conflicts of Interest: The authors declare no conflict of interest.

References

1. Armand, M.; Tarascon, J.-M. Building better batteries. *Nature* **2008**, *451*, 652–657. [CrossRef] [PubMed]
2. Hasoun, J.; Panero, S.; Reale, P.; Scrosati, B. A new, safe, high-rate and high-energy polymer lithium-ion battery. *Adv. Mater.* **2009**, *21*, 4807–4810. [CrossRef] [PubMed]
3. Chen, C.H.; Xie, S.; Sperling, E.; Yang, A.S.; Henriksen, G.; Amine, K. Stable lithium-ion conducting perovskite lithium-stronsium-tantalum-zirconium-oxide system. *Solid State Ion.* **2004**, *167*, 263–272. [CrossRef]
4. Thangadurai, V.; Weppner, W. $Li_6ALa_2Ta_2O_{12}$ (A = Sr, Ba): Novel garnet-like oxides for fast lithium ion conduction. *Adv. Funct. Mater.* **2005**, *15*, 107–112. [CrossRef]
5. Thangadurai, V.; Kaack, H.; Weppner, W. Novel fast lithium ion conduction in garnet-type $Li_5La_3M_2O_{12}$ (M. = Nb, Ta). *J. Am. Ceram. Soc.* **2003**, *86*, 437–440. [CrossRef]
6. Thangadurai, V.; Weppner, W. Investigations on electrical conductivity and chemical compatibility between fast lithium ion conducting garnet-like $Li_6BaLa_2Ta_2O_{12}$ and lithium battery cathodes. *J. Power Sources* **2005**, *142*, 339–344. [CrossRef]
7. Murugan, R.; Thangadurai, V.; Weppner, W. Effect of lithium ion content on the lithium ion conductivity of the garnet-like structure $Li_{5+x}BaLa_2Ta_2O_{11.5+0.5x}$ (x = 0 − 2). *Appl. Phys. A* **2008**, *91*, 615–620. [CrossRef]
8. Murugan, R.; Thangaduraiand, V.; Weppner, W. Lithium ion conductivity of $Li_{5+x}Ba_xLa_{3-x}Ta_2O_{12}$ (x = 0 − 2) with garnet-related structure in dependence of the barium content. *Ionics* **2007**, *13*, 195–203. [CrossRef]
9. Murugan, R.; Thangaduraiand, V.; Weppner, W. Lattice parameter and sintering temperature dependence of bulk and grain-boundary conduction of garnet-like solid Li-electrolytes. *J. Electrochem. Soc.* **2008**, *155*, A90–A101. [CrossRef]
10. Awaka, J.; Kijima, N.; Takahashi, Y.; Hayakawa, H.; Akimoto, J. Synthesis and crystallographic studies of garnet-related lithium-ion conductors $Li_6CaLa_2Ta_2O_{12}$ and $Li_6BaLa_2Ta_2O_{12}$. *Solid State Ion.* **2009**, *180*, 602–606. [CrossRef]

11. Zhong, Y.; Zhou, Q.; Guo, Y.; Li, Z.; Qiang, Y. The ionic conductivity of $Li_6BaLa_2M_2O_{12}$ with coexisting Nb and Ta on the M sites. *Ionics* **2013**, *19*, 697–700. [CrossRef]
12. Kokal, I.; Ramanujachary, K.V.; Notten, P.H.L.; Hintzen, H.T. Sol-gel synthesis and lithium ion conduction properties of garnet-type $Li_6BaLa_2Ta_2O_{12}$. *Mater. Res. Bull.* **2012**, *47*, 1932–1935. [CrossRef]
13. Baral, A.K.; Narayanan, S.; Ramezanipour, F.; Thangadurai, V. Evaluation of fundamental transport properties of Li-excess garnet-type $Li_{5+2x}La_3Ta_{2-x}Y_xO_{12}$ (x = 0.25, 0.5 and 0.75) electrolytes using ac impedance and dielectric spectroscopy. *Phys. Chem. Chem. Phys.* **2014**, *16*, 11356–11365. [CrossRef] [PubMed]
14. Gao, Y.X.; Wang, X.P.; Wang, W.G.; Fang, Q.F. Sol-gel synthesis and electrical properties $Li_5La_3Ta_2O_{12}$ lithium ionic conductors. *Solid State Ion.* **2010**, *181*, 33–36. [CrossRef]
15. Cussen, E.J. The structure of lithium garnets: Cation disorder and clustering in a new family of fast Li^+ ion conductors. *Chem. Commun.* **2006**, *4*, 412–413. [CrossRef]
16. O'Challaghan, M.P.; Cussen, E.J. Lithium dimer formation in the Li-conducting garnets $Li_{5+x}Ba_xLa_{3-x}Ta_2O_{12}$ ($0 < x \leq 1.6$). *Chem. Commun.* **2007**, *20*, 2048–2050.
17. Xu, M.; Park, M.S.; Lee, J.M.; Kim, T.Y.; Park, Y.S.; Ma, E. Mechanisms of Li^+ transport in garnet-type cubic $Li_{3+x}La_3M_2O_{12}$ (M. = Te, Nb, Zr). *Phys. Rev. B* **2012**, *85*, 052301. [CrossRef]
18. Murugan, R.; Thangadurai, V.; Weppner, W. Fast Lithium ion conduction in garnet-type $Li_7La_3Zr_2O_{12}$. *Angew. Chem. Int. Ed.* **2007**, *46*, 7778. [CrossRef]
19. Bernstein, N.; Johannes, M.D.; Hoang, K. Origin of the structural phase transition in $Li_7La_3Zr_2O_{12}$. *Phys. Rev. Lett.* **2012**, *109*, 205702. [CrossRef]
20. Rangasamy, E.; Wolfenstine, J.; Sakamoto, J. The role of Al and Li concentration on the formation of cubic garnet solid electrolyte of nominal composition $Li_7La_3Zr_2O_{12}$. *Solid State Ion.* **2012**, *206*, 28. [CrossRef]
21. Buannic, L.; Orayech, B.; López Del Amo, J.-M.; Carrasco, J.; Katcho, N.A.; Aguesse, F.; Manalastas, W.; Zhang, W.; Kilner, J.; Llordes, A. Dual substitution strategy to enhance Li^+ ionic conductivity in $Li_7La_3Zr_2O_{12}$ solid electrolyte. *Chem. Mater.* **2017**, *29*, 1769. [CrossRef]
22. Rettenwander, D.; Redhammer, G.; Preishuber-Pflugl, F.; Cheng, L.; Miyara, L.; Wagner, R.; Welzl, A.; Suard, E.; Doeff, M.M.; Wilkening, M.; et al. Structural and electrochemical consequences of Al and Ga cosubstitution in $Li_7La_3Zr_2O_{12}$ solid electrolytes. *Chem. Mater.* **2016**, *28*, 2384. [CrossRef] [PubMed]
23. Deviannapoorani, C.; Dhivya, L.; Ramakumar, S.; Murugan, R. Lithium ion transport properties of high conductive tellurium substituted $Li_7La_3Zr_2O_{12}$ cubic lithium garnets. *J. Power Sources* **2013**, *240*, 18. [CrossRef]
24. Luo, Y.; Li, X.; Chen, H.; Guo, L. Influence of sintering aid on the microstructure and conductivity of the garnettype W-doped $Li_7La_3Zr_2O_{12}$ ceramic electrolyte. *J. Mater. Sci. Mater. Electron.* **2019**, *30*, 17195. [CrossRef]
25. Wang, C.; Lin, P.P.; Gong, Y.; Liu, Z.G.; Lin, T.S.; He, P. Co-doping effects of Ba^{2+} and Ta^{5+} on the microstructure and ionic conductivity of garnet-type solid state electrolytes. *J. Alloys Compd.* **2021**, *854*, 157143. [CrossRef]
26. Han, J.; Zhu, J.; Li, Y.; Yu, X.; Wang, S.; Wu, G.; Xie, H.; Vogel, S.C.; Izumi, F.; Momma, K.; et al. Experimental visualization of of lithium conduction pathways in garnet-type $Li_7La_3Zr_2O_{12}$. *Chem. Commun.* **2012**, *48*, 9840. [CrossRef]
27. Wang, D.; Zhong, G.; Dolotko, O.; Li, Y.; McDonald, M.J.; Mi, J.; Fu, R.; Yang, Y. The synergistic effects of Al and Te on the structure and Li+-mobility of garnet-type solid electrolytes. *J. Mater. Chem. A* **2014**, *2*, 20271. [CrossRef]
28. Izumi, F.; Ikeda, T. A Rietveld-Analysis Programm RIETAN-98 and Its Applications to Zeolites. *Mater. Sci. Forum.* **2000**, *321–324*, 198–205. [CrossRef]
29. Almond, D.P.; Ducan, G.K.; West, A.R. The determination of hopping rates and carrier concentrations in ionic conductors by a new analysis of ac conductivity. *Solid State Ion.* **1983**, *8*, 159–164. [CrossRef]
30. Ahmad, M.M.; Yamada, K. Hopping rates and concentration of mobile fluoride ions in $Pb_{1-x}Sn_xF_2$ solid solutions. *J. Chem. Phys.* **2007**, *127*, 124507. [CrossRef]
31. Hairetdinov, E.F.; Uvarov, N.F.; Patel, H.K.; Martin, S.W. Estimation of the free-charge-carrier concentration in fast-ion conducting Na_2S-B_2S_3 glasses from as analysis of the frequency-dependent conductivity. *Phys. Rev. B* **1994**, *50*, 13259–13266. [CrossRef] [PubMed]
32. Ghosh, A.; Pan, A. Scaling of the conductivity spectra in ionic glasses: Dependence on the structure. *Phys. Rev. Lett.* **2000**, *84*, 2188. [CrossRef] [PubMed]
33. Adams, S.; Rao, R.P. Ion transport and phase transition in $Li_{7-x}La_3(Zr_{2-x}M_x)O_{12}$ (M = Ta^{5+}, Nb^{5+}, x = 0, 0.25). *J. Mater. Chem.* **2012**, *22*, 1426–1434. [CrossRef]
34. Ramirez, A.P.; Subramanian, M.A.; Gardel, M.; Blumberg, G.; Li, D.; Vogt, T.; Shapiro, S.M. Giant dielectric constant response in a copper-titanate. *Solid State Commun.* **2000**, *115*, 217–220. [CrossRef]
35. Li, M.; Sinclair, D.C.; West, A.R. Extrinsic origins of the apparent relaxorlike behavior in $CaCu_3Ti_4O_{12}$ ceramics at high temperatures: A cautionary tale. *J. Appl. Phys.* **2011**, *109*, 084106. [CrossRef]
36. Ahmad, M.M.; Kotb, H.M.; Joseph, C.; Kumar, S.; Alshoaibi, A. Transport and dielectric properties of mechanosynthesized $La_{2/3}Cu_3Ti_4O_{12}$ ceramics. *Crystals* **2021**, *11*, 313. [CrossRef]

37. Garcia-Martin, S.; Morata-Orrantia, A.; Alario-Franco, M.A. Influence of the crystal microstructure on the dielectric response of the $La_{0.67}Li_{0.2}Ti_{0.8}Al_{0.2}O_3$. *J. Appl. Phys.* **2006**, *100*, 054101. [CrossRef]
38. Ahmad, M.M. Giant dielectric properties of nanocrystalline $Pb_{1-x}Sn_xF_2$ solid solutions. *J. Mater. Sci. Mater. Electron.* **2014**, *25*, 4398–4403. [CrossRef]